Relationship between the cell thickness and the optimum period of textured back reflectors in thin-film microcrystalline silicon solar cells

Hitoshi Sai (齋 均),[1,a)] Kimihiko Saito (齊藤 公彦),[2] Nana Hozuki (保月なな),[2] and Michio Kondo (近藤 道雄)[1]
[1]*Research Center for Photovoltaic Technologies, National Institute of Advanced Industrial Science and Technology (AIST), Central 2, Umezono 1-1-1, Tsukuba, Ibaraki 305-8568, Japan*
[2]*Photovoltaic Power Generation Technology Research Association (PVTEC), Tsukuba 305-8568, Japan*

(Received 14 November 2012; accepted 24 January 2013; published online 8 February 2013)

Periodically textured back reflectors with hexagonal dimple arrays are applied to thin-film microcrystalline silicon (μc-Si:H) solar cells. When the textures have a moderate aspect ratio, the optimum period for obtaining a high short circuit current density (J_{SC}) is found to be equal to or slightly larger than the cell thickness. If the cell thickness exceeds the texture period, the cell surface tends to be flattened and texture-induced defects are generated, which constrain the improvement in J_{SC}. Based on these findings, we have fabricated optimized μc-Si:H cells achieving a high efficiency exceeding 10% and a J_{SC} of 30 mA/cm^2. © *2013 American Institute of Physics*. [http://dx.doi.org/10.1063/1.4790642]

Thin-film silicon solar cells (TFSSCs) are a promising candidate for the future large-area photovoltaic systems operating in the gigawatt scale because of the abundance and non-toxicity of the source materials.[1,2] However, further conversion efficiency improvement is desirable to make TFSSC more cost-competitive. In TFSSC, so-called light trapping technology is crucial to absorb photons within thin Si films to compensate for their insufficient carrier transport properties and comparatively higher film deposition cost. For this purpose, textured substrates have been implemented to scatter the incident light and elongate the optical path length inside the cells.[1–22]

In recent years, periodically textured substrates or surface gratings have been actively studied as a more sophisticated platform with a potential for realizing a higher current density than is realized with the conventional textures having randomness.[9–21] Because of their simplicity and uniformity in texture morphology, periodic structures have the possible advantage of much clearer correlations between texture structures and the photovoltaic performance in solar cells. In addition, the periodicity allows us to use periodic boundary conditions in optical simulations, which reduce the calculation cost substantially. The higher potential benefit of periodic textures was demonstrated in hydrogenated amorphous Si (a-Si:H) solar cells.[9] More recently, our group reported that a carefully chosen periodic texture enhances the conversion efficiency as well as the current density in microcrystalline Si (μc-Si:H) solar cells.[14] In that report, periodically textured substrates with hexagonal dimple arrays (hereafter, "honeycomb texture") were developed and applied to 1-μm-thick μc-Si:H cells in order to determine an optimum texture for light trapping.[14] In addition, the results of some 2-μm-thick cells suggested that the optimum period could be dependent on the cell thickness.[15] However, our results were not clearly conclusive, because of the limited data obtained. In this letter, we investigate the correlation between texture parameters such as period and the performance of solar cells in more detail with an additional parameter, namely, cell thickness, using substrate-type *n-i-p* μc-Si:H solar cells. We show that the period of textures must be modified based on thickness, for higher efficiency and current density. Based on our findings, we optimize the periodic textures for each cell thickness. Accordingly, a high short circuit current density (J_{SC}) exceeding 30 mA/cm^2 and a high efficiency of 10.7% are obtained.

Honeycomb textures were fabricated by the following procedure. First, a hexagonal photo-resist pattern was formed on a Si wafer with a thermally grown SiO_2 film using photolithography. Next, the wafer was soaked in a diluted buffered HF (BHF) solution to transfer the hexagonal pattern onto the SiO_2 film. After the removal of the remaining resist, a Ag/ZnO:Ga stacked film (200 nm/100 nm) was deposited on the honeycomb-textured SiO_2 layer by sputtering, to obtain a highly reflective and conductive surface. In this work, we fabricated honeycomb substrates with periods of $P = 1.0$ to 4.0 μm and aspect ratios of $H/P = 0.2$ to 0.25, where H denotes the peak height of the texture. As reported previously, we found that this range of H/P gives the highest J_{SC} in 1-μm-thick μc-Si:H cells.[14]

Substrate-type *n-i-p* μc-Si:H cells with an active area of 1 cm^2 were fabricated on these substrates. The structure of the solar cell consists of honeycomb-textured substrate/Ag/ZnO/μc-Si:H n-i-p layers/In_2O_3:Sn (ITO, 70 nm)/Ag grid. The intrinsic μc-Si:H layer was deposited with conventional plasma-enhanced chemical vapor deposition (PECVD) using SiH_4/H_2 gas mixture, with the thickness t_i varying from 0.5 to 3 μm. The n-type and p-type μc-Si:H were also deposited by PECVD using PH_3 and B_2H_6 as dopant gases, respectively. For some solar cells, wide-gap nanocrystalline silicon oxides (nc-SiO_X:H) were applied in the doped layers for reducing the absorption loss.[5] The top ITO film and Ag finger grid electrodes were deposited by sputtering at room temperature. Isolation of the cells was done by reactive ion etching. Finally, all the cells were annealed at 175 °C for 2 h. The performance of the cells was evaluated by measuring

a)Author to whom correspondence should be addressed. Electronic mail: hitoshi-sai@aist.go.jp.

current-voltage (J-V) characteristics with a dual-light solar simulator under AM 1.5 G 100 mW/cm^2 and external quantum efficiency (EQE) spectra. Reflectivity of the cells was also investigated using a spectrometer with an integral sphere (Perkin Elmer, Lambda 950).

Figures 1(a)–1(c) show the scanning electron microscope (SEM) images of a honeycomb-textured substrate with $P = 1.5\ \mu$m and $H/P = 0.23$, and a 1-μm-thick μc-Si:H solar cell deposited on it. The sides of the dimples on the substrate can be tapered in a manner similar to a crater, as shown in Fig. 1(a), by properly utilizing the so-called undercut effect during BHF etching. This feature is advantageous to avoid the generation of defects, which are often grown at steep valleys on textured substrates.[22] As seen in Fig. 1(b), the morphology of the cell surface is not a simple replication of the substrate. The diameter of each dimple is reduced after μc-Si:H film growth, and tiny holes are left behind on the cell surface. This can be also confirmed in Fig. 1(c), showing a cross-sectional view of the cell.

The texture period giving the highest J_{SC} is dependent on the cell thickness. Figure 2 shows the relationship between the period of honeycomb-textured substrates and the J_{SC} of μc-Si:H solar cells with $t_i = 0.5$, 1, 2, and 3 μm. Although here we fixed the H/P in the range of 0.2–0.25, the series of data is plotted only at periods of 1.4 μm and 1.5 μm to show the variation caused by changing H/P from 0.05 to 0.25. The J_{SC} obtained by utilizing quasi-periodically textured Al substrates[12] is plotted as supplemental data in the range of $P < 1\ \mu$m. As shown in Fig. 2, the optimum period providing the highest J_{SC} becomes longer with increasing cell thickness. In the case of $t_i = 0.5\ \mu$m, the optimum period is found to be around 1 μm, although a clear peak is not observable due to the lack of experimental data in the range $P < 1\ \mu$m. A high J_{SC} of over 30 mA/cm^2 is attained at $P = 3$ to 4 μm for cells with $t_i = 3\ \mu$m and a (p)nc-SiO$_X$ layer. These results, summarized in Fig. 2, show that the cell thickness must be taken into account to design optimum periodic surface textures for light trapping in TFSSCs, at least when using moderate aspect ratios.

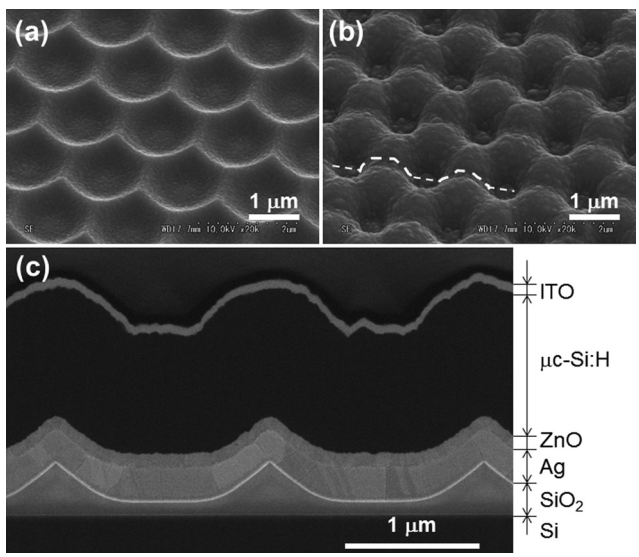

FIG. 1. SEM images of a 1-μm-thick μc-Si:H solar cell fabricated on a honeycomb textured substrate with a period of 1.5 μm: (a) the substrate surface, (b) the cell surface, and (c) the cross section along the dashed line depicted in (b). (a) and (b) were taken at an inclination angle of 45°.

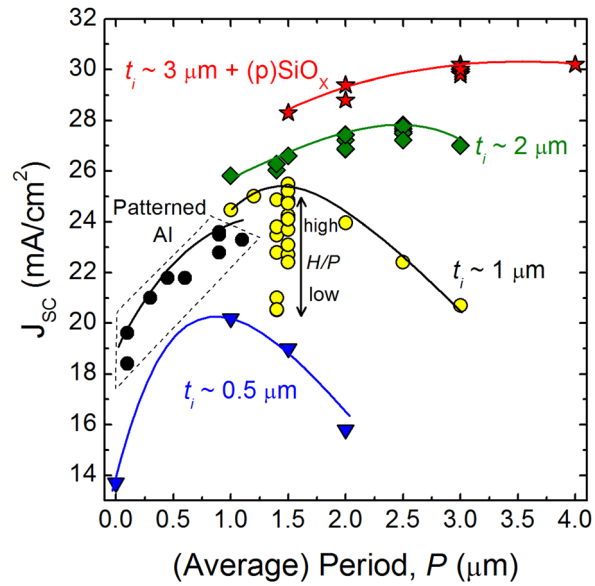

FIG. 2. The relationship between the period of textured substrates and the J_{SC} of μc-Si:H solar cells with i-layer thicknesses of $t_i = 0.5$, 1, 2, and 3 μm. For cells with $t_i = 3\ \mu$m, a wide-gap (p)nc-SiO$_X$ layer was applied. Circles surrounded by dashed lines represent data obtained with 1-μm-thick cells on patterned Al substrates fabricated by anodic oxidation (see Ref. 13). Solid lines in this figure are guides to the eye.

Spectral properties of μc-Si:H cells on honeycomb substrates vary drastically with changing cell thickness. In Fig. 3, we compare the EQE and absorption spectra of the μc-Si:H cells fabricated on honeycomb textures with $P = 1.5$

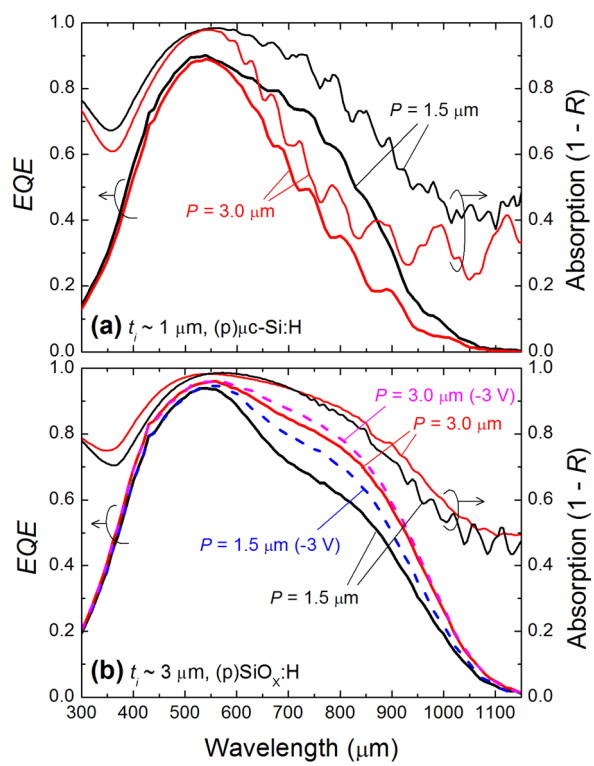

FIG. 3. EQE and absorption (1-R) spectra of μc-Si:H solar cells fabricated on textured substrates with P = 1.5 and 3.0 μm. (a) $t_i = 1\ \mu$m and (b) $t_i = 3\ \mu$m. EQE spectra obtained under a negative bias voltage of −3 V are shown by the dashed lines in (b).

and 3 μm. Recently reported theoretical and numerical works have shown that optimal light trapping occurs when the grating period approximately equals the target wavelength, which in our case is 0.8 to 1 μm.[20,21] Based on this information, the texture with $P = 1.5$ μm can be expected to outperform that with $P = 3$ μm. In fact, in the case of 1-μm-thick cells, the texture with $P = 1.5$ μm shows a substantial enhancement in EQE as well as in absorption for wavelengths in the range of 600–1100 nm, as plotted in Fig. 3(a), indicating better light confinement within the cell. The EQE in the short wavelength region is also slightly improved, owing to the anti-reflection effect achieved by the rough front textures, as shown in Fig. 1(b). Contrastively, in the case of 3-μm thick cells, the texture with $P = 3.0$ μm exhibits higher absorption than the other across the entire wavelength region shown in the figure. The difference between $P = 1.5$ μm and 3.0 μm was more pronounced in the EQE spectra. A negative bias voltage applied during the EQE measurement especially helps the carrier collection in the case of $P = 1.5$ μm, as plotted in Fig. 3(b). This means that the texture with $P = 1.5$ μm induces more carrier recombination centers than the other, within thick cells.

As seen in Fig. 3(b), the origin of the lower J_{SC} in the 3-μm-thick cell on the texture with $P = 1.5$ μm has two components: optical loss and carrier collection loss. Taking into account the fact that the same texture exhibits an excellent light trapping in 1-μm-thick cells, as shown in Fig. 3(a), the lower optical absorption in this case should be ascribed to the front texture. It was reported that an increase in the thickness causes the flattening of the cell surface and the deterioration of the light scattering ability of the TFSSC deposited on textured substrates.[8] To confirm this, we characterize the front texture of the fabricated cells by atomic force microscopy using root-mean square roughness σ_{RMS} as a figure of merit. Figure 4 shows the ratio of σ_{RMS} of the cell surface to that of the substrate surface, σ_{RMS}(cell)/σ_{RMS}(substrate), as a function of cell thickness. The σ_{RMS} ratio becomes smaller than unity when the cell surface is flattened with respect to the substrate surface. In fact, the σ_{RMS} ratio decreases when t_i increases beyond a certain limit. The threshold thickness is dependent on the period of the substrates: a longer period of the substrate results in a larger threshold thickness. At this threshold thickness, the flat bottom areas of the concaves on the cell surface, as seen in Fig. 1(c), almost disappear. When compared with Fig. 2, the threshold thickness in each period roughly corresponds to the optimum thickness that gives the highest J_{SC} for the period. Thus, our results confirm that the surface flattening must be avoided for enhancing photon absorption in conventional TFSSCs, in which a Si thin film is deposited on textured substrates.

Next, we consider the carrier collection loss observed in the 3-μm-thick cells. Figure 5 shows the current densities, which are denoted as $J_{EQE}(-6\,\mathrm{V})$ and J_{SC}, calculated from EQE curves measured under a negative bias voltage of -6 V, as functions of P. It is clearly seen that the difference between $J_{EQE}(-6\,\mathrm{V})$ and J_{SC} reduces with increasing P, meaning that the density of recombination centers in the cell is suppressed. The difference between $P = 1.5$ and 3.0 μm is reduced from 1.7 to 0.6 mA/cm^2 by applying negative bias voltages. The remaining difference, 0.6 mA/cm^2, can be regarded as an optical loss, assuming perfect carrier collection under this condition.

To gain a deeper insight into the origin of the carrier collection loss, we observed the microstructure of the cells by high-angle angular dark-field scanning transmission electron microscopy (HAADF-STEM). Figure 6 shows cross sectional bright-field TEM images of the 3-μm-thick μc-Si:H cells. In the case of $P = 1.5$ μm, bright streaky parts can be observed underneath the concaves on the cell surface, as shown in Fig. 6(a). The bright streak, which is composed of a low-density amorphous structure, starts to grow roughly in the middle of the cell and ends with a void at the cell surface. Note that, as seen in this figure, the void is filled with the carbon used for the preparation of TEM samples. The low-density part is more clearly seen in the HAADF image in Fig. 6, as a dark line. We ascribe these low-density parts to the occurrence of the shadowing effect at the bottom of the concaves, which is very likely to occur when the cell becomes thicker than the threshold thickness mentioned above. These parts are essentially identical to the so-called "cracks" reported by other groups,[22] and contain a large number of defects that enhance carrier recombination.

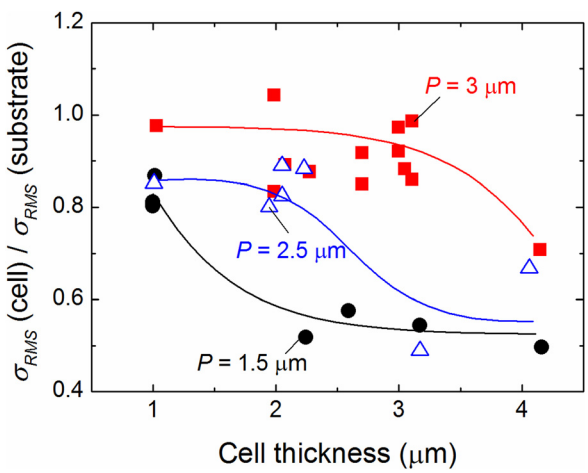

FIG. 4. The roughness ratio of the cell surface to the substrate surface as functions of the thickness of μc-Si:H cells fabricated on honeycomb textures with periods of 1.5, 2.5, and 3 μm. Solid lines are guides to the eye.

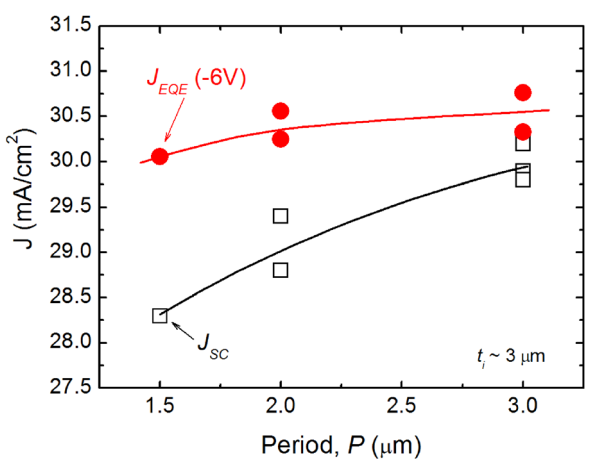

FIG. 5. J_{SC} and J_{EQE} (-6 V) of the 3-μm-thick μc-Si:H cells fabricated on honeycomb-textured substrates as functions of the period. The solid lines are guides to the eye.

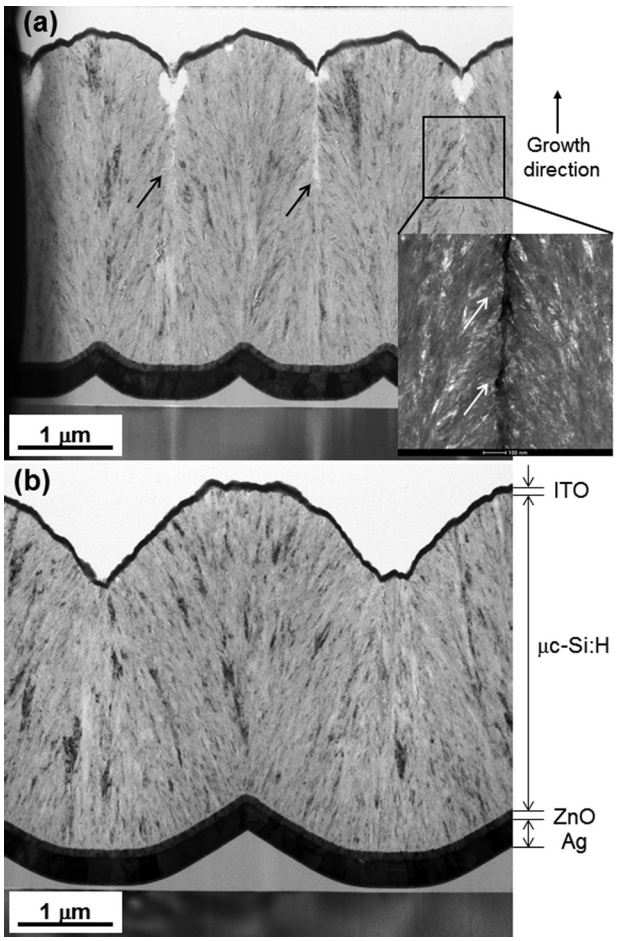

FIG. 6. Bright-field STEM images of 3-μm-thick μc-Si:H cells on honeycomb-textured substrates with (a) P = 1.5 μm and (b) P = 3 μm. Black arrows in (a) indicate low-density defective parts that exist in the upper half of the cell. A magnified HAADF image is shown in the inset in panel (a) to show the low-density part (seen as a dark line) more clearly.

Moreover, the non-uniform coverage of the p-layer around the concaves could weaken the internal electric field. All these effects can cause insufficient carrier collection and a reduction in J_{SC}. Contrastively, in the case of $P = 3\,\mu$m, no clear defective parts are found within the entire μc-Si:H layer, as is evident from Fig. 6(b). This result confirms that the enlarged dimples mitigate the severe shadowing effect and resulting carrier collection problems in thicker cells.

Finally, the *J-V* properties of the most efficient μc-Si:H solar cells fabricated in this study are summarized in Table I. By using properly chosen honeycomb textures with respect to the cell thickness and more transparent doped layers, we have realized active area efficiencies of 10.3% and 10.7% in the cells with $t_i = 1$ and 2 μm, respectively. These are among the highest efficiencies reported thus far for single-junction μc-Si:H cells with periodic textures. The EQE and absorption spectra of the highest-efficiency cell reported herein are plotted in Fig. 7. In addition, a J_{SC} of 30 mA/cm^2 has been achieved for the cell with $t_i = 3\,\mu$m, which is comparable to the highest-current cell with state-of-the-art random textures.[7] However, the effect of the decrease in open circuit voltage V_{OC} and fill factor *FF* surpasses that of the gain in J_{SC}, and the efficiency declines. This detrimental effect against achieving a much higher efficiency may be mitigated by using improved textures, doped layers, buffer layers, and i-layers.

TABLE I. *J-V* parameters of μc-Si:H cells fabricated on a flat and honeycomb textures. All the cells have an active area of 1 cm^2.

Substrate	t_i (μm)	p-layer	n-layer	V_{OC} (V)	J_{SC} (mA/cm^2)	FF	Efficiency (%)
Flat	1	μc-Si	μc-Si	0.539	17.5	0.742	7.0
P = 1.5 μm	1	SiO_X	SiO_X	0.519	26.7	0.746	10.3
P = 2.5 μm	2	SiO_X	SiO_X	0.510	28.7	0.732	10.7
P = 3 μm	3	SiO_X	μc-Si	0.500	30.1	0.693	10.4

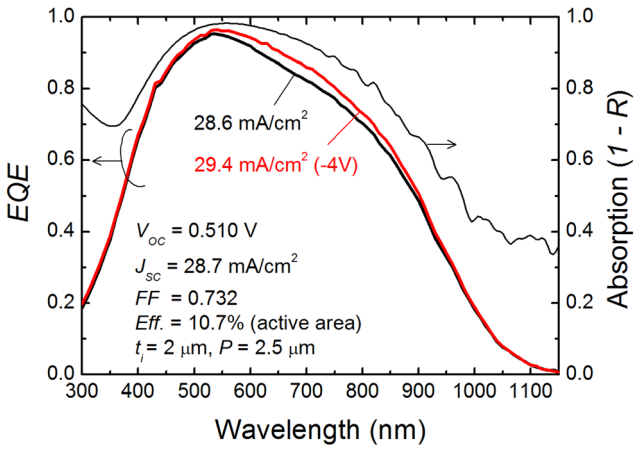

FIG. 7. EQE and absorption spectra of the highest-efficiency cell obtained in this study.

To summarize, we have investigated the interplay between the period of the textures and the thickness of the μc-Si:H cells by using back reflectors with honeycomb textures. It is found that the optimum period for obtaining a high J_{SC} as well as high efficiency requires to be equal to or slightly larger than the cell thickness. This can be explained by the following mechanisms: When the cell thickness exceeds the texture period, J_{SC} is limited by (i) deteriorated light trapping in the cell due to the surface flattening, and (ii) generation of defects due to texture-induced shadowing effect during Si deposition. If the texture period is excessively long, the light-trapping effect becomes weaker and the J_{SC} is decreased, as predicted by optical simulations. We emphasize here that such clear correlations between the cell thickness and the texture period are obtained by utilizing periodic structures. Based on the findings described above, we have optimized the honeycomb texture and achieved an active area efficiency of 10.7% in a 2-μm-thick cell and a J_{SC} of 30 mA/cm^2 in a 3-μm-thick cell, indicating a high potential advantage for periodic textures. Application of theoretically optimum textures to TFSSC would require the use of new approaches, such as those involving flattened substrates[23,24] or post-deposition texturing, to avoid constraints that normally accompany the growth of Si films on textured substrates.

This work was supported by New Energy and Industrial Technology Development Organization (NEDO), Japan. Photolithography process was conducted at the AIST Nano-Processing Facility, supported by "Nanotechnology Network Japan" of the Ministry of Education, Culture, Sports, Science and Technology (MEXT), Japan.

[1]J. Meier, S. Dubail, R. Platz, P. Torres, U. Kroll, J. A. Anna Selvan, N. Pellaton Vaucher, Ch. Hof, D. Fischer, H. Keppner, R. Flückiger, A. Shah, V. Shklover, and K.-D. Ufert, Sol. Energy Mater. Sol. Cells **49**, 35 (1997).
[2]K. Yamamoto, T. Suzuki, M. Yoshimi, and A. Nakajima, Jpn. J. Appl. Phys., Part 2 **36**, L569 (1997).
[3]M. Kambe, A. Takahashi, N. Taneda, K. Masumo, T. Oyama, and K. Sato, in *Proceedings of 33rd IEEE Photovoltaics Specialist Conference, San Diego*, 2008, pp. 609–613.
[4]W. W. Wenas, A. Yamada, M. Konagai, and K. Takahashi, Jpn. J. Appl. Phys., Part 2 **30**, L441 (1991).
[5]M. Despeisse, C. Battaglia, M. Boccard, G. Bugnon, M. Charrière, P. Cuony, S. Hänni, L. Löfgren, F. Meillaud, G. Parascandolo, T. Söderström, and C. Ballif, Phys. Status Solidi A **208**, 1863 (2011).
[6]M. Berginski, J. Hüpkes, M. Schulte, G. Schöpe, H. Steibig, B. Rech, and M. Wuttig, J. Appl. Phys. **101**, 074903 (2007).
[7]B. Yan, G. Yue, L. Sivec, J. Owens-Mawson, J. Yang, and S. Guha, Sol. Energy Mater. Sol. Cells **104**, 13 (2012).
[8]H. Sai, H. Jia, and M. Kondo, J. Appl. Phys. **108**, 044505 (2010).
[9]C. Battaglia, C.-M. Hsu, K. Söderström, J. Escarre, F.-J. Haug, M. Charrière, M. Boccard, M. Despeisse, D. T. L. Alexander, M. Cantoni, Y. Cui, and C. Ballif, ACS Nano **6**, 2790 (2012).
[10]K. Söderström, F.-J. Haug, J. Escarré, O. Cubero, and C. Ballif, Appl. Phys. Lett. **96**, 213508 (2010).
[11]F.-J. Haug, T. Söderström, M. Python, V. Terrazzoni-Daudrix, X. Niquille, and C. Ballif, Sol. Energy Mater. Sol. Cells **93**, 884 (2009).
[12]H. Sai and M. Kondo, J. Appl. Phys. **105**, 094511 (2009).
[13]M. Vanecek, O. Babchenko, A. Purkrt, J. Holovsky, N. Neykova, A. Poruba, Z. Remes, J. Meier, and U. Kroll, Appl. Phys. Lett. **98**, 163503 (2011).
[14]H. Sai, K. Saito, and M. Kondo, Appl. Phys. Lett **101**, 173901 (2012).
[15]H. Sai, K. Saito, and M. Kondo, IEEE J. Photovoltaics **3**, 5 (2013).
[16]C. Haase and H. Stiebig, Appl. Phys. Lett. **91**, 061116 (2007).
[17]A. Čampa, J. Krč, and M. Topič, J. Appl. Phys. **105**, 083107 (2009).
[18]R. Dewan, I. Vasilev, V. Jovanov, and D. Knipp, J. Appl. Phys. **110**, 013101 (2011).
[19]X. Sheng, J. Liu, I. Kozinsky, A. M. Agarwall, J. Michel, and L. C. Kimerling, Adv. Mater. **23**, 843 (2011).
[20]Z. Yu, A. Raman, and S. Fan, Opt. Express **18**, A366 (2010).
[21]S. E. Han and G. Chen, Nano Lett. **10**, 4692 (2010).
[22]M. Python, O. Madani, D. Dominé, F. Meillaud, E. Vallat-Sauvain, and C. Ballif, Sol. Energy Mater. Sol. Cells **93**, 1714 (2009).
[23]H. Sai, Y. Kanamori, and M. Kondo, Appl. Phys. Lett. **98**, 113502 (2011).
[24]K. Söderstrom, G. Bugnon, F.-J. Haug, S. Nicolay, and C. Ballif, Sol. Energy Mater. Sol. Cells **101**, 193 (2012).